



Exact Solution for Free Vibration Analysis of FGM Beams

Mohamed Bouamama^{1*}, Abbes Elmeiche¹, Abdelhak Elhennani¹, Tayeb Kebir², Zine El Abidine Harchouche²

¹Laboratory Mechanics of Structures and Solids, Department of Mechanical Engineering, Faculty of Technology, University of Sidi Bel Abbes, Sidi Bel Abbes 22000, Algeria

²Laboratory of Materials and Systems Reactive, Department of Mechanical Engineering, Faculty of Technology, University of Sidi Bel Abbes, Sidi Bel Abbes 22000, Algeria

Corresponding Author Email: mohamed.bouamama@univ-sba.dz

<https://doi.org/10.18280/rcma.300201>

ABSTRACT

Received: 18 November 2019

Accepted: 6 January 2020

Keywords:

exact solution, free vibration analysis, beams, E-FGM, fundamental frequencies, material distribution

This study relates the exact solution for free-vibration analysis of beams in material gradient (FGMs) subjected to the different conditions of support using the Euler Bernoulli theory (CBT). It is assumed that the material properties continuously change across the thickness of the beam according to the exponential function (E-FGM). The equations of motion are obtained by applying the principle of virtual works on beams and fundamental frequencies are found by solving the equations governing the eigenvalue problems. Numerical results are presented to describe the influence of the material on the fundamental frequencies of the beam for different state boundaries.

1. INTRODUCTION

Improving the performance of the structural parts can lead to search, in the same material, different properties, often antagonistic, but locally optimized. The development of composite materials has made it possible to associate specific properties of different materials within the same room.

Improving the performance of the structural parts can lead to search, in the same material, different properties, often antagonistic, but locally optimized. The development of composite materials has made it possible to associate specific properties of the different materials within the same room.

Gradient property materials (FGMs) can be produced by continually changing the material components in a predetermined profile. The most distinct characteristics of the FGM micro-structure materials are their non-uniform with graded properties, macro in space. It is designed to improve and optimize the characteristic thermoelectric mechanical structures for sealing micro and nano [1].

Most of the FGM families are gradually made of metal-refractory ceramics. Typically, FGMs are constructed from a mixture of ceramic and metal or a combination of different materials. Ceramic in an FGM provides a barrier of thermal effects and protects the metal against corrosion and oxidation, and the FGM is hard and reinforced by the metallic composition. Currently FGMs are developed for general use as structural elements in extremely high temperature environments and different applications.

Due to the wide application of FGM several studies have been conducted on the mechanical and thermal behavior of FGMs [2-12]. Detailed theoretical and experimental studies have been carried out and published, on the mechanics of rupture [13-15], the distribution of thermal stresses [16-24], the treatment [25-27], etc. Among these FGM structures, beams have always remained the interests of researchers

because of their applications. Approaches such as the use of shear deformation theory of beams, energy method, and the finite element method were performed.

The aim of this work is to analyze the free vibrations of FGM beams subjected to the different support conditions using the Euler Bernoulli (CBT) theory. It is assumed that the material properties continuously change across the thickness of the beam according to the exponential function (E-FGM). Solutions are found by solving equilibrium equations for eigenvalue problems.

2. MATERIAL PROPERTIES OF E-FGM BEAMS

Many researchers use the exponential function to describe the material properties to describe the material properties of FGM materials. The exponential function is given by Delale and Erdogan [28].

$$E(z) = A e^{\beta(z+h/2)} \quad (1)$$

With:

$$A = E_1 \text{ and } \beta = \frac{1}{h} \ln \frac{E_1}{E_2} \quad (2)$$

where, E_2 and E_1 are respectively the material properties (Young's modulus; density or Poisson's ratio) of the lower surface ($z = -h/2$) and the upper surface ($z = +h/2$) of the E-FGM beam.

The variation of the Young's modulus through the thickness of the E-FGM beam is presented in Figure 1. The Young modulus is varied using a single function that dominates the material distribution in the E-FGM beam.

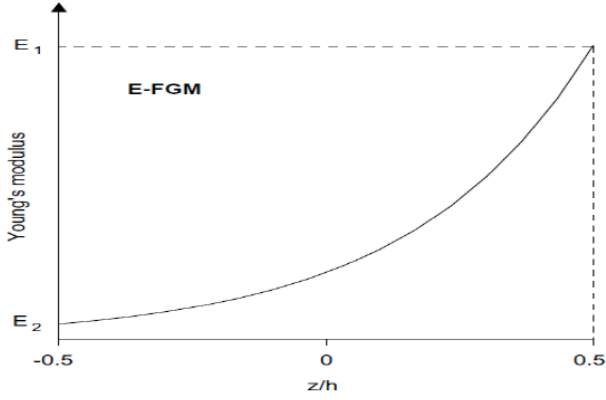


Figure 1. The variation of the Young's modulus of the E-FGM beam

3. MATHEMATICAL FORMULATIONS

Consider an FGM beam having the dimensions shown in Figure 2 subjected to free transverse vibration. It is assumed that the beam has a linear elastic behavior and the displacements following the axes "x" and "z" of an arbitrary point in the beam and denoted respectively by $u(x, z, t)$ and $w(x, z, t)$. This study is based on the classical theory of beam (CTB). The displacement field of any point of the beam takes the following form:

$$U(M) = \begin{cases} u(x, z, t) = u(x, t) - z \frac{\partial w(x, t)}{\partial x} \\ w(x, z, t) = w(x, t) \end{cases} \quad (3)$$

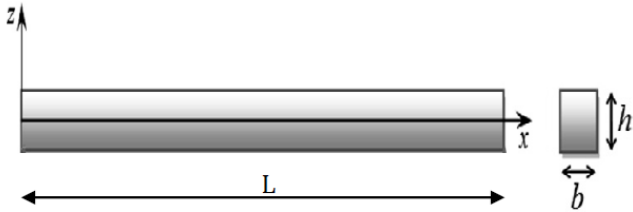


Figure 2. Coordinates and geometry of the E-FGM beam

where, $U(M)$ is the displacement field of a point "M"; $u(x, t)$ and $w(x, t)$ are the displacement components on the median plane. The relationship strain constraints can be written in matrix form as follows:

$$\begin{Bmatrix} \sigma_{xx} \\ \sigma_{zz} \\ \tau_{xz} \end{Bmatrix} = \begin{bmatrix} \frac{E(z)}{1-\nu(z)^2} & 0 & 0 \\ 0 & \frac{E(z)}{1-\nu(z)^2} & 0 \\ 0 & 0 & \frac{E(z)}{2(1+\nu(z))} \end{bmatrix} \begin{Bmatrix} \epsilon_{xx} \\ \epsilon_{zz} \\ \gamma_{xz} \end{Bmatrix} \quad (4)$$

Such as:

The strain tensor is defined as follows:

$$\begin{aligned} \epsilon_{xx} &= \frac{\partial u(x, z, t)}{\partial x} = \frac{\partial u(x, t)}{\partial x} - z \frac{\partial^2 w(x, t)}{\partial x^2} \\ \epsilon_{zz} &= \frac{\partial w(x, z, t)}{\partial z} = \frac{\partial w(x, t)}{\partial z} \\ \gamma_{xz} &= \frac{\partial u(x, z, t)}{\partial z} + \frac{\partial w(x, z, t)}{\partial x} \end{aligned} \quad (5)$$

Using the virtual work principle on the E-FGM beam, the resulting equations of motion are:

$$\begin{cases} A_{11} \frac{\partial^2 u_0(x, t)}{\partial x^2} - B_{11} \frac{\partial^3 w(x, t)}{\partial x^3} = 0 \\ B_{11} \frac{\partial^3 u_0(x, t)}{\partial x^3} - D_{11} \frac{\partial^4 w(x, t)}{\partial x^4} + I_1 \ddot{w}(x, t) = 0 \end{cases} \quad (6)$$

With:

$$\begin{aligned} (A_{11}, B_{11}, D_{11}) &= \int_{-\frac{h}{2}}^{+\frac{h}{2}} \frac{E(z)}{1-\nu(z)^2} (1, z, z^2) dz \\ I_1 &= \int_{-\frac{h}{2}}^{+\frac{h}{2}} \rho(z) dz \end{aligned}$$

4. MATHEMATICAL SOLUTIONS

Analytical solutions are obtained from Eq. (6), keeping the same E-FGM beam geometry for different boundary conditions (S-S, C-C, C-S, C-F). For harmonic vibrations, the vertical displacement can be expressed:

$$w(x, t) = w(x) e^{i\omega_n t} \quad (7)$$

The general amplitude equation is described as follows:

$$\begin{aligned} w_n(\tau) &= A_1 \cdot \cos(\beta_n L \tau) + A_2 \cdot \sin(\beta_n L \tau) + \\ &A_3 \cdot \cosh(\beta_n L \tau) + A_4 \cdot \sinh(\beta_n L \tau) \end{aligned} \quad (8)$$

Such as:

$$\tau = \frac{x}{L} \quad \tau \in [0, 1]$$

A_1, A_2, A_3 and A_4 are arbitrary parameters determine and β_n is the associated wave number to the n th own mode. In this study we consider the beams with four different modes of support that is to say, one beam clamped in the two extremities (C-C), a second beam articulated in extremity and clamped in other (C-S), third beam articulated to extremities (S-S), and a fourth beam clamped in extremity and free in other (C-F).

The four boundary conditions can be obtained as follows:

a. C-C: Clamped-clamped beam

$$\begin{cases} w_n(\tau) = w_n'(\tau) = 0 & \tau = 0 \\ w_n(\tau) = w_n'(\tau) = 0 & \tau = 1 \end{cases} \quad (8.a)$$

b. C-S: Clamped-supported beam

$$\begin{cases} w_n(\tau) = w_n'(\tau) = 0 & \tau = 0 \\ w_n(\tau) = w_n''(\tau) = 0 & \tau = 1 \end{cases} \quad (8.b)$$

For each mode, the natural frequencies are given by:

$$\omega_n = \left(\frac{B_n}{L} \right)^2 \sqrt{\xi}$$

c. S-S: Supported-supported beam

$$\begin{cases} w_n(\tau) = w_n''(\tau) = 0 & \tau = 0 \\ w_n(\tau) = w_n''(\tau) = 0 & \tau = 1 \end{cases} \quad (8.c)$$

where,

$$\xi = \frac{1}{I_1} \left(\frac{B_{11}^2}{A_{11}} - D_{11} \right)$$

d. C-F: Clamped-free beam

$$\begin{cases} w_n(\tau) = w_n'(\tau) = 0 & \tau = 0 \\ w_n(\tau) = w_n'''(\tau) = 0 & \tau = 1 \end{cases} \quad (8.d)$$

5. NUMERICAL APPLICATION

Using Eq. (7) for the four types of boundary conditions we obtain equations with eigenvalues, for the problem of free vibration:

$$([K] - \lambda_n [M]) \{A\} = 0$$

Such as:

$$\lambda_n = \left(\frac{\beta_n}{L} \right)^4$$

For the solutions of the Eq. (6), the following determinant could be equal to zero:

$$\det([K] - \lambda_n [M]) = 0$$

In this study, we assume that the E-FGM beam is made of a mixture of ceramic and metal whose composition varies across the thickness. As the upper facet i.e., at $(z = h/2)$ is made of 100% ceramic Al_2O_3 (alumina), while the lower facet $(Z = -h/2)$ is made in 100% Al metal (Aluminum). The mechanical properties of these two materials are:

Ceramic (Alumina, Al_2O_3): $EC = 380 \times 10^9 \text{ N/m}^2$; $\nu = 0.33$; $\rho_C = 3800 \text{ kg/m}^3$.

Metal (Aluminium, Al): $EM = 70 \times 10^9 \text{ N/m}^2$; $\nu = 0.33$; $\rho_M = 2780 \text{ kg/m}^3$.

The numerical results are presented in terms of dimensionless frequencies. The non-dimensional natural frequencies parameter is defined as:

$$\bar{\omega}_n = \omega_n L^2 \sqrt{\frac{\rho_c A}{E_c I}}$$

Knowing that: I is the inertia moment and A is the section of FGM beam.

Table 1. Comparison of the fundamental frequencies $\bar{\omega}_n$ for isotropic beams

| BCs | Source | $\bar{\omega}_1$ | $\bar{\omega}_2$ | $\bar{\omega}_3$ | $\bar{\omega}_4$ | $\bar{\omega}_5$ |
|-----|------------------------------|------------------|------------------|------------------|------------------|------------------|
| C-C | Present (exact solution) | 22.3733 | 61.6728 | 120.903 | 199.859 | 298.556 |
| | (Eltaher et al.) [29] | 22.4926 | 63.2455 | 107.762 | 128.924 | 208.792 |
| C-S | Present (exact solution) | 15.4182 | 49.9649 | 104.248 | 178.270 | 272.031 |
| | (Eltaher et al.) [29] | 15.4937 | 51.0507 | 107.961 | 110.069 | 204.300 |
| S-S | Present (exact solution) | 9.8696 | 39.4784 | 88.8264 | 157.914 | 246.740 |
| | (Eltaher et al.) [29] | 9.8698 | 39.5500 | 89.6055 | 107.868 | 162.459 |
| C-F | Present (exact solution) | 3.5160 | 22.0345 | 61.6972 | 120.902 | 199.860 |
| | (Eltaher et al.) [29] | 3.5228 | 22.3641 | 53.9884 | 108.971 | 130.773 |

Table 2. The first three frequencies $\bar{\omega}_n$ of E-FGM beam for $L/h = 10$

| E_U/E_L | $\bar{\omega}_n$ | C-C | C-S | S-S | C-F |
|-----------|------------------|--------|--------|--------|--------|
| 1 | $\bar{\omega}_1$ | 22.373 | 15.418 | 9.8696 | 3.5160 |
| | $\bar{\omega}_2$ | 61.673 | 49.964 | 39.478 | 22.034 |
| | $\bar{\omega}_3$ | 120.90 | 104.24 | 88.826 | 61.697 |
| 2 | $\bar{\omega}_1$ | 22.108 | 15.235 | 9.7525 | 3.4743 |
| | $\bar{\omega}_2$ | 60.942 | 49.373 | 39.010 | 21.773 |
| | $\bar{\omega}_3$ | 119.47 | 103.01 | 87.773 | 60.966 |
| 3 | $\bar{\omega}_1$ | 21.720 | 14.968 | 9.5813 | 3.4133 |
| | $\bar{\omega}_2$ | 59.871 | 48.505 | 38.325 | 21.391 |
| | $\bar{\omega}_3$ | 117.37 | 101.20 | 86.231 | 59.895 |
| 4 | $\bar{\omega}_1$ | 21.352 | 14.714 | 9.4190 | 3.3555 |
| | $\bar{\omega}_2$ | 58.857 | 47.684 | 37.676 | 21.028 |
| | $\bar{\omega}_3$ | 115.38 | 99.488 | 84.771 | 58.880 |
| 5 | $\bar{\omega}_1$ | 21.020 | 14.486 | 9.2726 | 3.3033 |
| | $\bar{\omega}_2$ | 57.941 | 46.942 | 37.090 | 20.702 |
| | $\bar{\omega}_3$ | 113.59 | 97.942 | 83.454 | 57.965 |

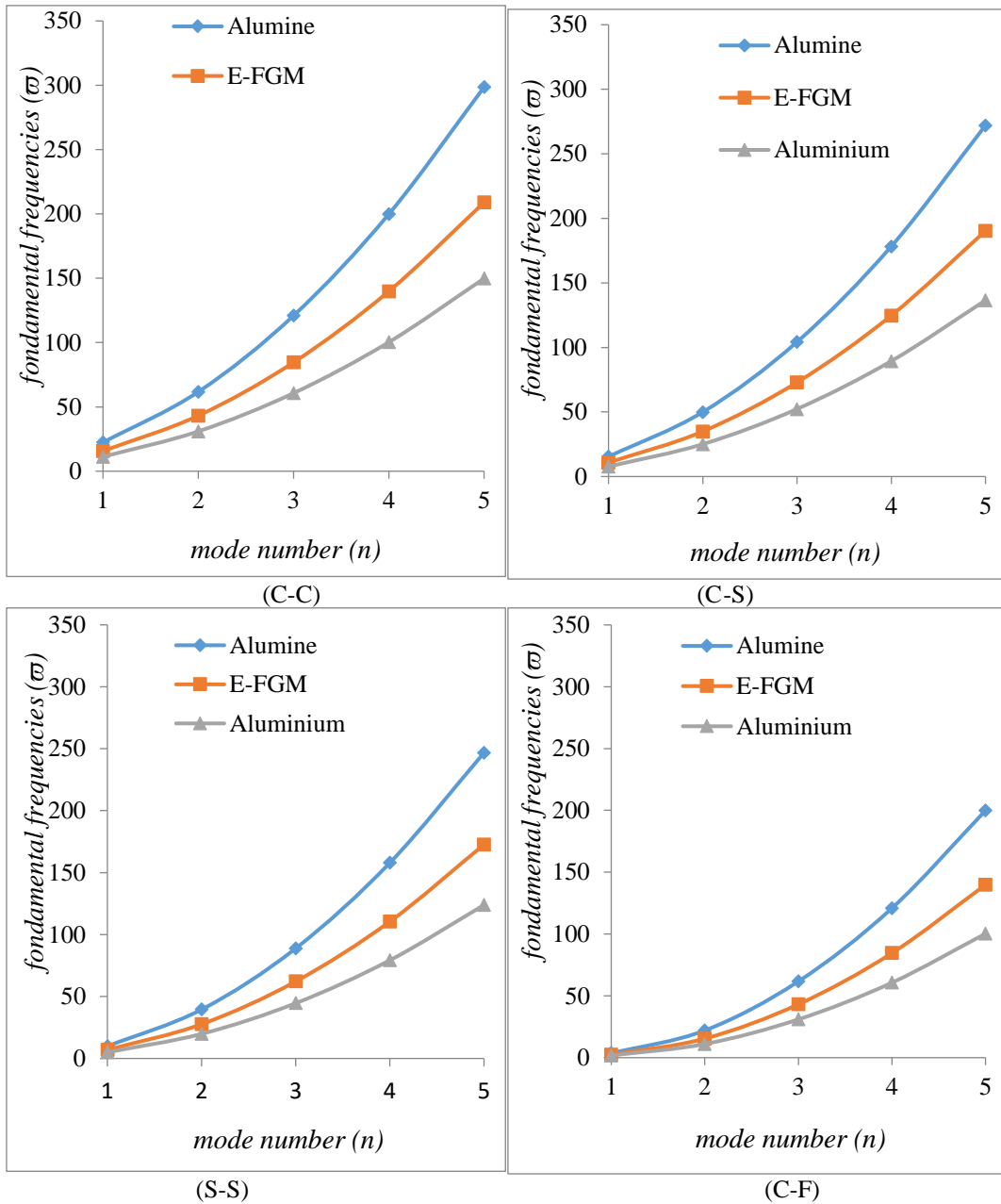


Figure 3. The fundamental frequencies of an E-FGM beam for different conditions of support with a ceramic-metal mixture

To verify the accuracy of this method, the non-dimensional frequencies of the FGM beam with different boundary conditions were compared by Eltahir et al. [29]. The results are shown in the Table 1. We can notice that the results were in a good agreement that demonstrated the precision of our model.

Table 2 shows the first three fundamental frequencies ($\bar{\omega}_n$) Of an E-FGM beam, for different boundary conditions with stiffness ratios $E_U/E_L = 1, 2, 3, 4$ and 5.

It may be noted that the most important fundamental frequencies are those of the isotropic and homogeneous beams. ($E_U/E_L = 1$) Where the mixture is made of pure ceramic (100% Alumina). It is also observed that the fundamental frequencies of an E-FGM beam decrease with the increase in stiffness ratio which is due to the decrease in the amount of ceramic in the mixture.

Figure 3 shows the proportionality of the fundamental frequencies with the vibratory modes (n) of the E-FGM beams and compared with those of isotropic and homogeneous beams which describes the two basic materials (Ceramics, Metal).

From these figures, it can be deduced that the change in the fundamental frequencies depends on the combination of the volume fraction (E-FGM) of the extreme materials. This frequency change is influenced by the stiffness of the beams and becomes very significant for higher vibratory modes.

6. CONCLUSION

In this paper, we have analyzed the exact solution for free vibrations of the beams by using the classical Euler-Bernoulli theory (CBT) and assuming that the material properties of the beam are evaluated continuously in the direction of thickness according to the exponential law (E-FGM). The aim of this paper is to see the influence of the material distribution of the two extreme materials on the fundamental frequencies of the system. Numerical results have been presented for the E-FGM beam with various boundary states. These results can be used as a reference to other numerical methods.

REFERENCES

- [1] Nguyen, T.K., Nguyen, T.T.P., Vo, T.P., Thai, H.T. (2015). Vibration and buckling analysis of functionally graded sandwich beams by a new higher-order shear deformation theory. *Composites Part B: Engineering*, 76: 273-285. <https://doi.org/10.1016/j.compositesb.2015.02.032>
- [2] Shen, H.S. (2007). Thermal postbuckling behavior of shear deformable FGM plates with temperature-dependent properties. *International Journal of Mechanical Sciences*, 49(4): 466-478. <https://doi.org/10.1016/j.ijmecsci.2006.09.011>
- [3] Tounsi, A., Houari, M.S.A., Benyoucef, S., Adda Bedia, E.A. (2013). A refined trigonometric shear deformation theory for thermoelastic bending of functionally graded sandwich plates. *Aerospace Science and Technology*, 24(1): 209-220. <https://doi.org/10.1016/j.ast.2011.11.009>
- [4] Gayen, D., Roy, T. (2014). Finite element based vibration analysis of functionally graded spinning shaft system. *Proceedings of the Institution of Mechanical Engineers, Part C: Journal of Mechanical Engineering Science*, 228(18): 3306-3321. <https://doi.org/10.1177/0954406214527923>
- [5] Şimşek, M. (2015). Bi-directional functionally graded materials (BDFGMs) for free and forced vibration of timoshenko beams with various boundary conditions. *Composite Structures*, 133: 968-978. <https://doi.org/10.1016/j.compstruct.2015.08.021>
- [6] Naebe, M., Shirvanimoghaddam, K. (2016). Functionally graded materials: A review of fabrication and properties. *Applied Materials Today*, 5: 223-245. <https://doi.org/10.1016/j.apmt.2016.10.001>
- [7] Ebrahimi, F., Ghasemi, F., Salari, E. (2016). Investigating thermal effects on vibration behavior of temperature-dependent compositionally graded Euler beams with porosities. *Meccanica*, 51(1): 223-249. <https://doi.org/10.1007/s11012-015-0208-y>
- [8] Elmeiche, A., Megueni, A., Lousdad, A. (2016). Free vibration analysis of functionally graded Nanobeams based on different order beam theories using Ritz method. *Periodica Polytechnica Mechanical Engineering*, 60(4): 209-219. <http://dx.doi.org/10.3311/PPme.8707>
- [9] Shaw, S. (2017). Mechanical behavior of a functionally graded rectangular plate under transverse load: A cosserat elasticity analysis. *Journal of Failure Analysis and Prevention*, 17(4): 690-698. <http://dx.doi.org/10.1007/s11668-017-0292-5>
- [10] Zaoui, F.Z., Hanifi, H.A., Abderahman, L.Y., Mustapha, M.H., Abdelouahed, T., Djamel, O. (2017). Free vibration analysis of functionally graded beams using a higher-order shear deformation theory. *Mathematical Modelling of Engineering Problems*, 4(1): 7-12. <https://doi.org/10.18280/mmep.040105>
- [11] Elhannani, A., Refassi, K., Elmeiche, A., Bouamama, M. (2019). Vibration analysis of functionally graded tapered rotor shaft system. *Mechanics and Mechanical Engineering*, 23(1): 241-245. <https://doi.org/10.2478/mme-2019-0032>
- [12] Bouamama, M., Elmeiche, A., Elhennani, A., Kebir, T. (2019). Dynamic stability analysis of functionally graded timoshenko beams with internal viscous damping distribution. *Journal Européen des Systèmes Automatisés*, 52(4): 341-346. <http://dx.doi.org/10.18280/jesa.520402>
- [13] Bao, G., Wang, L. (1995). Multiple cracking in functionally graded ceramic/metal coatings. *International Journal of Solids and Structures*, 32(19): 2853-2871. [https://doi.org/10.1016/0020-7683\(94\)00267-Z](https://doi.org/10.1016/0020-7683(94)00267-Z)
- [14] Marur, P.R. (1999). *Fracture Behaviour of Functionally Graded Materials*, Ph. D. dissertation, Auburn University, Alabama.
- [15] Shojaee, S., Daneshmand, A. (2015). Crack analysis in media with orthotropic functionally graded materials using extended isogeometric analysis. *Engineering Fracture Mechanics*, 147: 203-227. <http://dx.doi.org/10.1016/j.engfracmech.2015.08.025>
- [16] Williamson, R.L., Rabin, B.H., Drake, J.T. (1993). Finite element analysis of thermal residual stresses at graded ceramic-metal interfaces. Part I. Model description and geometrical effects. *Journal of Applied Physics*, 74(2): 1310-1320. <http://dx.doi.org/10.1063/1.354910>
- [17] Boukhari, A., Boukhelf, F., Benbakhti, A.D., Bachir, B.M., Tounsi, A., Adda Bedia, E.A. (2016). The thermal study of wave propagation in functionally graded material plates (FGM) based on neutral surface position. *Mathematical Modelling of Engineering Problems*, 3(4): 202-205. <https://doi.org/10.18280/mmep.030410>
- [18] Daikh, A.A., Megueni, A. (2018). Thermal buckling analysis of functionally graded sandwich plates. *Journal of Thermal Stresses*, 41(2): 139-159. <http://dx.doi.org/10.1080/01495739.2017.1393644>
- [19] Kettaf, F.Z., Houari, M.S.A., Benguediab, M., Tounsi, A. (2013). Thermal buckling of functionally graded sandwich plates using a new hyperbolic shear displacement model. *Steel and Composite Structures*, 15(4): 399-423. <http://dx.doi.org/10.12989/scs.2013.15.4.399>
- [20] Noda, N. (1999). Thermal stresses in functionally graded materials. *Journal of Thermal Stresses*, 22(4-5): 477-512. <http://dx.doi.org/10.1080/014957399280841>
- [21] Ohmichi, M., Noda, N. (2016). Steady thermal stresses in functionally graded eccentric polygonal cylinder with circular hole. *Archive of Applied Mechanics*, 86(6): 1163-1177. <http://dx.doi.org/10.1007/s00419-015-1085-5>
- [22] Burlayenko, V.N., Altenbach, H., Sadowski, T., Dimitrova, S.D., Bhaskar, A. (2017). Modelling functionally graded materials in heat transfer and thermal stress analysis by means of graded finite elements. *Applied Mathematical Modelling*, 45: 422-438. <http://dx.doi.org/10.1016/j.apm.2017.01.005>
- [23] Li, D., Deng, Z., Chen, G., Ma, T. (2018). Mechanical and thermal buckling of exponentially graded sandwich plates. *Journal of Thermal Stresses*, 41(7): 883-902. <http://dx.doi.org/10.1080/01495739.2018.1443407>
- [24] Khosravi, A., Akbari, A., Bahreinizad, H., Bani, M.S., Karimi, A. (2017). Optimizing through computational modeling to reduce dogboning of functionally graded coronary stent material. *Journal of Materials Science: Materials in Medicine*, 28(9): 142. <http://dx.doi.org/10.1007/s10856-017-5959-7>
- [25] Kesler, O., Finot, M., Suresh, S., Sampath, S. (1997). Determination of processing-induced stresses and properties of layered and graded coatings: Experimental method and results for plasma-sprayed Ni-Al₂O₃. *Acta*

Materialia, 45(8): 3123-3134.
[http://dx.doi.org/10.1016/S1359-6454\(97\)00015-3](http://dx.doi.org/10.1016/S1359-6454(97)00015-3)

[26] Shao, Z.S., Wang, T.J., Ang, K.K. (2007). Transient thermo-mechanical analysis of functionally graded hollow circular cylinders. Journal of Thermal Stresses, 30(1): 81-104.
<http://dx.doi.org/10.1080/01495730600897211>

[27] Hassan, A.H.A., Kurgan, N. (2019). A review on buckling analysis of functionally graded plates under thermo-mechanical loads. International Journal of Engineering & Applied Sciences, 11(1): 345-368.
<http://dx.doi.org/10.24107/ijeas.555719>

[28] Delale, F., Erdogan, F. (1983). The crack problem for a nonhomogeneous plane. Journal of Applied Mechanics, 50(3): 609. <http://dx.doi.org/10.1115/1.3167098>

[29] Eltaher, M.A., Alshorbagy, A.E., Mahmoud, F.F. (2013). Vibration analysis of Euler–Bernoulli nanobeams by using finite element method. Applied Mathematical Modelling, 37(1): 4787-4797.
<https://doi.org/10.1016/j.apm.2012.10.016>

NOMENCLATURE

L Total Length of beam, m

| | |
|---------------|---------------------------------|
| h | Thickness of the beam, m |
| b | Width of beam, m |
| E | Young's module, Gpa |
| A11, B11, D11 | Terms of rigidities |
| [M] | Mass matrix |
| [K] | Stiffness matrix |
| I_l | Function of the volume fraction |
| {A} | unit vector |
| B_n | Wave number |

Greek symbols

| | |
|--------------------|----------------------------------|
| ξ | Ratio of stiffness coefficients |
| ρ | Mass density, Kg.m ⁻³ |
| u | Displacement along the X axis |
| w | Displacement along the Z axis |
| \mathcal{E}_{ij} | Strain Tensor |
| v | Poisson coefficient |
| ω | Eigenfrequency of the FGM beam |